

# Strategic electromagnetic interferences suppression in boost converters: zero-switch techniques

Zakaria M'barki, Ali Ait Salih, Youssef Mejdoub, Kaoutar Senhaji Rhazi

Laboratory of Networks, Computer Science, Telecommunication, Multimedia (RITM), Higher School of Technology ESTC, Hassan II University, Casablanca, Morocco

## Article Info

### Article history:

Received Oct 18, 2023

Revised Feb 10, 2024

Accepted Mar 6, 2024

### Keywords:

Boost converter

Conducted electromagnetic interference

Electric vehicle systems

Electromagnetic compatibility

Zero current switching

Zero voltage switching

## ABSTRACT

This article delves into the growing demand for efficient power conversion technologies accompanying the rise in electric vehicle (EV) adoption. Boost converters, essential for increasing the battery pack voltage to propel EV motors, pose a challenge due to the electromagnetic interference (EMI) generated by the high switching frequency of power devices. To address this issue, practitioners employ zero-voltage switching (ZVS) and zero-current switching (ZCS) techniques. In this comparative study, we systematically evaluate the effectiveness of these soft switching techniques in reducing conducted EMI in boost converters designed for EV applications. The results illuminate the potential of both ZVS and ZCS in significantly mitigating EMI emissions when compared to conventional hard-switching methods. Notably, ZVS soft switching emerges as more efficient and effective, particularly under higher loads, while ZCS soft switching excels in reducing EMI at lighter loads. In conclusion, the study asserts that ZVS soft switching presents a more promising solution for curtailing conducted EMI in boost converters for EV applications, particularly in high-load scenarios. However, it underscores the importance of considering specific operational conditions when deciding between the two techniques.

*This is an open access article under the [CC BY-SA](https://creativecommons.org/licenses/by-sa/4.0/) license.*



## Corresponding Author:

Zakaria M'barki

Laboratory of Networks, Computer Science, Telecommunication, Multimedia (RITM)

Higher School of Technology ESTC, Hassan II University of Casablanca

Km 7 El Jadida Road-r.p.8, B.P. 20000, Casablanca, Morocco

Email: mbarki.ensem@gmail.com

## 1. INTRODUCTION

In recent years, the burgeoning demand for electric vehicles (EVs) has propelled substantial research and development in power electronics converters, imperative for managing the robust high-power requirements of these vehicles. The boost converter, integral to EV applications for elevating battery voltage, assumes a central role in this landscape [1], [2]. Despite their ubiquity across diverse industries, these converters generate pollution owing to rapid switching characterized by quasi-trapezoidal waveforms [3]. The primary objective of our research is to mitigate conducted electromagnetic stresses in a boost converter tailored for EV applications [4], [5]. The metal oxide semiconductor field effect transistor (MOSFET) in power switches induces disruptive emissions during turn-off and turn-on phases, propagating within the frequency band spanning [150 KHz, 1 GHz] [6]. Despite a concurrent increase in frequency aligned with the evolution of power electronic components, resulting in heightened power density, it precipitates reduced efficiency and heightened electromagnetic pollution [7].

To address this challenge, we propose the application of the soft switching technique, aimed at reducing power losses and attenuating voltage or current gradients, thereby contributing to enhanced

electromagnetic compatibility [8]–[10]. Additionally, techniques such as filtering and pseudo-random modulation are implemented to mitigate electromagnetic interference (EMI) from power converters [11], [12]. The application of pseudo-random modulation at the control level serves to disperse harmonic energy across a wide frequency range, and its integration with resonant switching holds promise for meeting electromagnetic compatibility (EMC) standards [13], [14].

This research builds upon antecedent investigations into mitigating EMI in power electronics converters. A focal point is the concept of soft switching, designed to minimize power losses during transitions, ensuring switches operate under conditions of near-zero voltage or current [15], [16]. Despite notable advancements, critics underscore challenges in control algorithms, heightened component stress, and potential trade-offs with pivotal performance metrics, including size, weight, and cost considerations [17]. While extant studies have commendably explored various soft-switching techniques for EMI mitigation, a discernible gap exists in the lack of comparative investigations scrutinizing zero-current switching (ZCS) and zero-voltage switching (ZVS) methods, particularly in boost converters tailored for EV applications. This research seeks to bridge this intellectual void, presenting a comprehensive comparative analysis elucidating the efficacy of ZCS and ZVS techniques in diminishing EMI for EV boost converters. The scope of the investigation extends beyond EMI levels alone, encompassing critical performance parameters such as efficiency, power loss, and switching frequency. Moreover, the study delves into the nuanced impacts arising from diverse operating conditions, including load current and switching frequency, on the EMI levels engendered by each technique. The anticipated outcomes of this research are poised to offer valuable insights for researchers and engineers engaged in the development of efficient and acoustically unobtrusive power electronics converters tailored specifically for the demanding milieu of EV applications. In summary, this research stands as a pivotal contributor to the ongoing evolution of advanced power electronics converters, poised to meet and surpass the evolving requisites of the burgeoning EV market.

## 2. BOOST CONVERTER: MODELING AND IMPLEMENTATION INSIGHTS

Boost converters play a critical role in the realm of EVs by elevating the battery voltage to align with the requirements of the motor controller. This study focuses on scrutinizing the voltage augmentation from 24 to 48 V within a conventional 48 V EV. This process involves a switching configuration with a freewheeling diode (HFA25TB60) and a high-frequency MOSFET transistor (IRFP460), as depicted in Figure 1. The MOSFET is controlled by a fixed-frequency  $F_s$  logic signal  $V_{GS}$ , with a designated duty cycle represented by  $D$ .

To achieve precise power regulation in diverse electrical applications, a pulse width modulation (PWM) signal is generated, a vital component in this context. When combined with a driver like the TLP250, this PWM signal is not only amplified but also electrically isolated, effectively governing the power device (MOSFET). The PWM signal, through adjusting pulse duration, facilitates output management. Simultaneously, the driver ensures accurate switching and provides protection to the field programmable gate arrays (FPGAs) board against high power circuit voltages. This collaborative interaction achieves efficient energy management and safeguards sensitive components from potential electrical interference. The development of the examined boost converter is directed towards aligning with the specifications elucidated in Table 1.

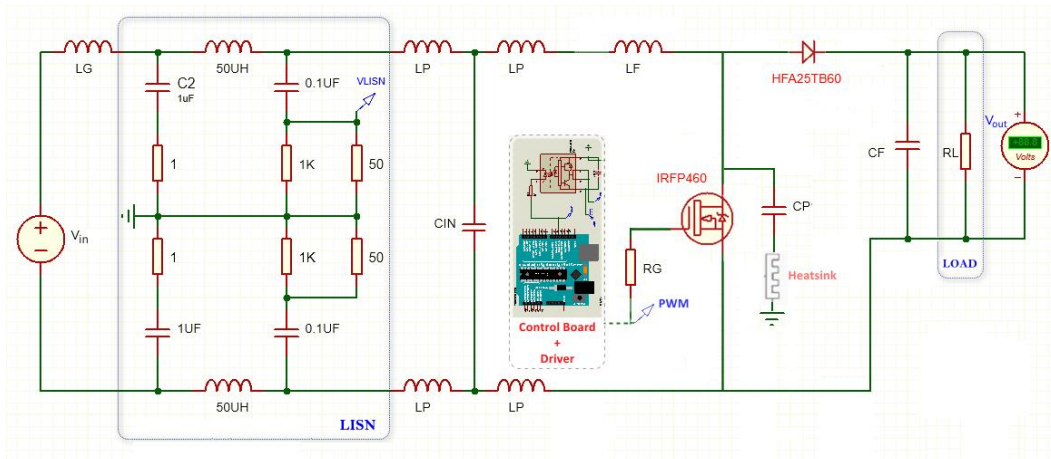


Figure 1. Boost converter: structure and EMI device measurements

Table 1. Simulation settings

Parameter	Normalized value	Units
1 Input voltage $V_{in}$	24	V
2 Output voltage $V_o$	48	V
3 Inductance $L_F$	150	uH
4 Capacitance $C_F$	10	uF
5 Load resistance $R_L$	12	$\Omega$
6 Input capacitance $C_{in}$	2.2	mF
7 Parasitic capacitor $C_p$	130	pF
8 Switching frequency $F_s$	100	KHz
9 Duty cycle D	0.5	---

### 3. SOFT SWITCHING IMPLEMENTATION STRATEGIES FOR ENHANCING BOOST CONVERTER PERFORMANCE

Soft switching, a fundamental technique in electrical systems, plays a crucial role in mitigating rapid voltage or current fluctuations within electronic setups, while concurrently suppressing conducted and radiated disturbances [18]–[20]. This involves integrating a damping circuit, such as a parallel capacitor (deployed in ZVS), to deliberately decelerate voltage transitions. Additionally, a series inductance (utilized in ZCS) is incorporated to judiciously temper current fluctuations during the intricate switching phase. Multiple soft switching configurations present versatile solutions, featuring: ZVS: this technique meticulously ensures that the voltage across the power switch, exemplified by a MOSFET transistor, meticulously maintains a state of zero during the intricate switching process, facilitating seamless transitions of electric current between states. (ZCS): ZCS, with precision, guarantees that the current coursing through the power switch assumes a state of zero at the precise moment of switching, orchestrating a harmonious transition of electrical voltage between distinct states. Both ZVS and ZCS, through their meticulous orchestration, demonstrate a discernible efficacy in the reduction of energy losses and disturbances intricately linked with sophisticated switching processes.

In a comprehensive panorama, the design of quasi-resonant converters operating at either zero voltage or zero current conspicuously manifests a set of distinctive characteristics:

- i. Normalized resonance frequency  $f_n = \frac{f_s}{f_r}$  with  $f_r = \frac{1}{2\pi\sqrt{L_R C_R}}$ .
- ii. Characteristic impedance  $Z_n = \sqrt{\frac{L_R}{C_R}}$ .
- iii. Normalized load resistance  $Q = \frac{R_L}{Z_n}$ .
- iv. Conversion ratio  $M = \frac{V_{out}}{V_{in}}$ .

#### 3.1. Soft switching: zero voltage switching

The scenario involves assuming that the inductance (L) and capacitance (C) of the filter significantly outweigh the inductance and capacitance of the resonance. As a result, the voltage source ( $V_{in}$ ) connected in series with inductance (L) is replaced with a direct current source ( $I_{in}$ ), and the output is simulated using a direct voltage source ( $V_o$ ). This concept is visually demonstrated in Figure 2. The operational configuration of the previously depicted boost converter is delineated into four modes (Figure 3), the four modes are linear (Figure 3(a)), resonance (Figure 3(b)), recovery (Figure 3(c)), and freewheeling (Figure 3(d)), each determined by the statuses of the primary switch and the freewheeling diode.

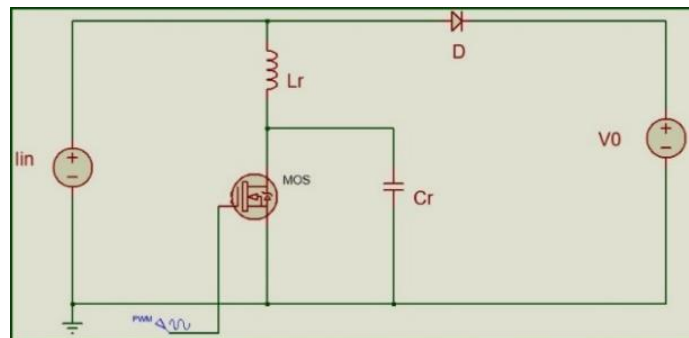


Figure 2. Schematic of the zero voltage switching quasi-resonant boost converter

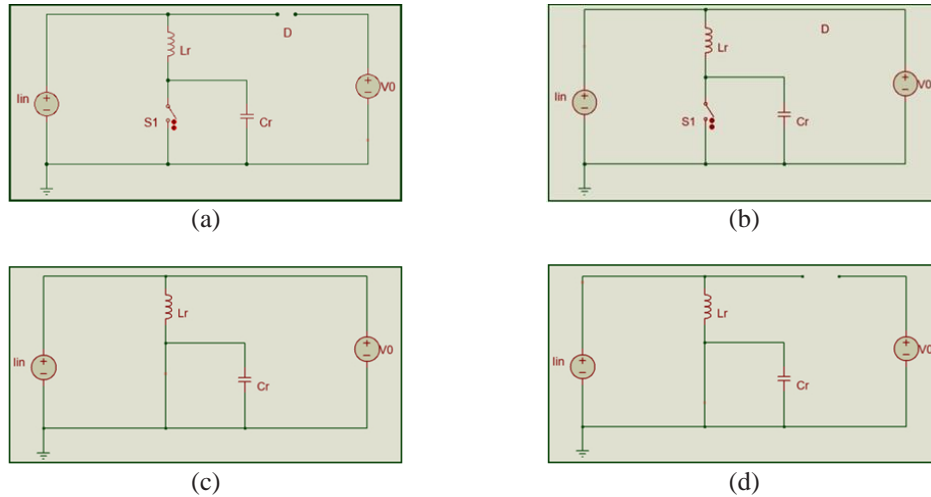


Figure 3. Equivalent circuits for (a) linear, (b) resonance, (c) recovery, and (d) freewheeling mode

Mode 1 [linear] ( $0 \leq t \leq t_1$ ): this mode is characterized initially by the charging of the capacitor  $C_r$ . This leads to (1) and (2):

$$i_{LR} = I_{in} \tag{1}$$

$$V_{CR} = \frac{I_{in}}{C_r} (t - t_0) \tag{2}$$

Mode 2 [resonance] ( $t_1 \leq t \leq t_2$ ): this mode commences when  $V_{CR}$  reaches  $V_o$ , at which point the voltage across diode D becomes positive. The inductor  $L_r$  and capacitor  $C_r$  are now in resonance. This leads to (3) and (4):

$$I_{LR}(t) = I_{in} \cdot \cos \omega_r (t - t_1) \tag{3}$$

$$V_{CR}(t) = V_o + Z_r \cdot I_{in} \cdot \sin \omega_r (t - t_1) \tag{4}$$

The strict conditions that should be satisfied:  $I_{in} \geq \frac{V_o}{Z_n}$

Mode 3 [recovery] ( $t_2 \leq t \leq t_3$ ): This mode is characterized by the end of resonance. Then,  $I_{LR}$  starts to increase linearly until reaching  $I_{in}$ . This leads to (5) and (6):

$$I_{LR}(t) = \frac{V_o}{L_r} (t - t_2) + I_{in} [1 + \cos \omega_r (t_2 - t_1)] \tag{5}$$

$$V_{CR}(t) = 0 \tag{6}$$

Mode 4 [freewheeling] ( $t_3 \leq t \leq T_s$ ): in this mode, the input current  $I_{in}$  is freewheeling through  $L_r$  and the main switch. This leads to (7) and (8):

$$I_{LR}(t) = I_{in} \tag{7}$$

$$V_{CR}(t) = 0 \tag{8}$$

At the end of this mode, at time  $t = T_s$ , the cycle repeats. The waveforms of the resonant tank are depicted in Figure 4. Figure 4 shows the current and voltage for the ZVS approach for control voltage (Figure 2(a))  $V_{gs}$ , inductor current  $I_{LR}$  (Figure 2(b)), and capacitive voltage  $V_{cr}$  (Figure 2(c)).

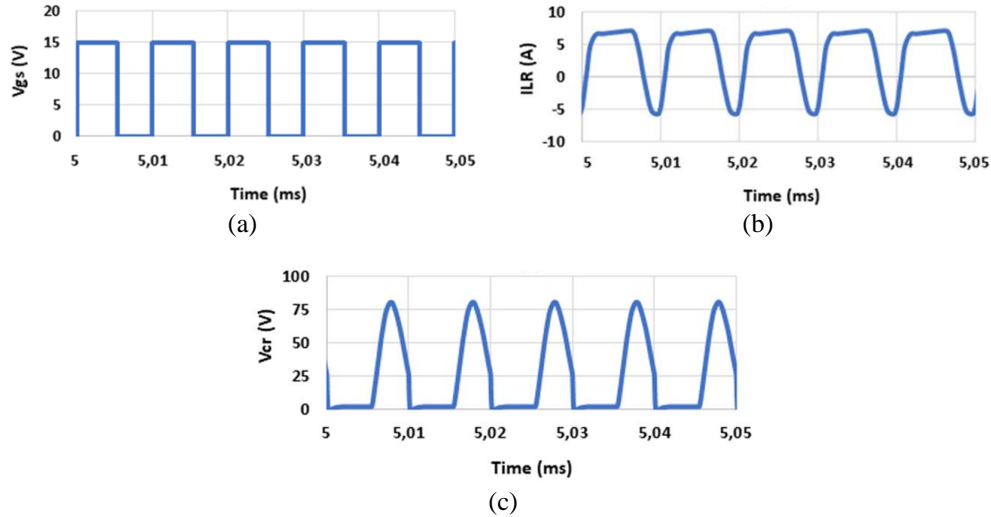


Figure 4. Current and voltage for the ZVS approach for (a) control voltage  $V_{gs}$ , (b) Inductor current  $I_{LR}$ , and (c) capacitive voltage  $V_{cr}$

The voltage conversion ratio,  $M$ , of the quasi-resonant ZVS converter can be expressed using the principle of energy conservation in the (9):

$$M = \left[ \frac{f_n}{2\pi} \left( \frac{Q}{2M} + \pi + \sin^{-1} \left( \frac{Q}{M} \right) + \frac{M}{Q} \left( 1 + \sqrt{1 - \left( \frac{Q}{M} \right)^2} \right) \right) \right]^{-1} \tag{9}$$

Thus, the plotting of the conversion ratio  $M$  against normalized frequency is conducted in this study for different load values  $Q$ . A numerical analysis technique, specifically the Newton-Raphson method, has been employed. The control characteristic illustrated in Figure 5 provides visual confirmation of these findings. Table 2 presents a summary of the ZVS-QRC parameters discussed earlier.

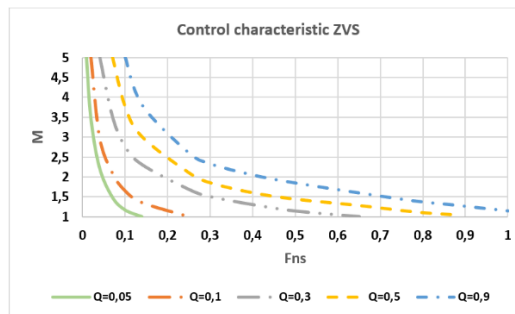


Figure 5. Conversion ratio characteristic as a function of normalized load

Table 2. Customizing the ZVS-QRC boost converter configuration

Parameter	Normalized value
Inductance $L_r$	4.7 $\mu$ H
Capacitance $C_r$	150 nF
Resonant frequency $F_r$	198 KHz
Duty cycle $D$	$\sim 0.54$

### 3.2. Soft switching: zero current switching

The assumptions from the previous section still hold, where the inductance ( $L$ ) and capacitance ( $C$ ) of the filter are considerably greater than the inductance and capacitance of the resonant elements. This is depicted in the illustrative Figure 6. The operational configuration of the previously modeled boost converter

is delineated into four modes (Figure 7), the four modes are linear (Figure 7(a)), resonance (Figure 7(b)), recovery (Figure 7(c)), and freewheeling (Figure 7(d)), each determined by the statuses of the primary switch and the freewheeling diode.

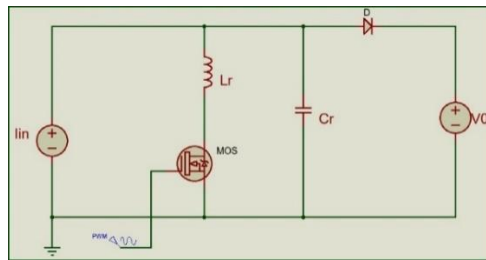


Figure 6. Schematic of the zero current switching quasi-resonant boost converter

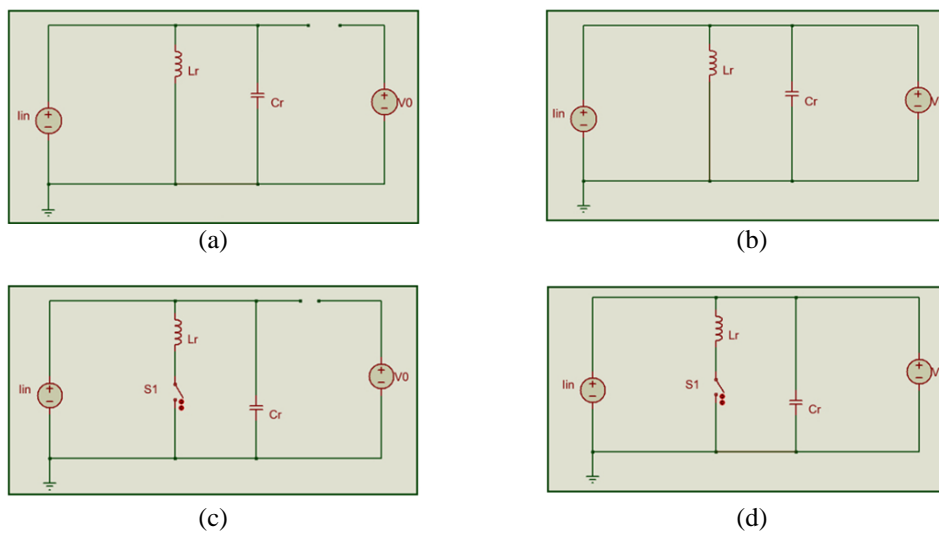


Figure 7. Equivalent circuits for (a) linear, (b) resonance, (c) recovery, and (d) freewheeling mode

Mode 1 [linear] ( $0 \leq t \leq t_1$ ): in this mode, when the main switch conducts at  $t_0$ , the diode D remains in its conducting state ( $L_r$  starts to store energy). This leads to (10) and (11):

$$i_{LR} = \frac{V_0}{L_r}(t-t_0) \tag{10}$$

$$V_{CR} = V_0 \tag{11}$$

Mode 2 [resonance] ( $t_1 \leq t \leq t_2$ ): this mode initiates when diode D stops conducting, causing  $L_r$  and  $C_r$  to start resonating. As a result, we derive the (12) and (13):

$$I_{LR}(t) = I_{in} + \frac{V_0}{Z_r} \sin w_r(t-t_1) \tag{12}$$

$$V_{CR}(t) = V_0 \cdot \cos w_r(t-t_1) \tag{13}$$

The strict conditions that should be satisfied:  $I_{in} \leq \frac{V_0}{Z_n}$

Mode 3 [recovery] ( $t_2 \leq t \leq t_3$ ): This mode is characterized by the end of resonance. Consequently, capacitor  $C_r$  begins to charge from the input current source  $I_{in}$ . As a result, the (14) and (15) are obtained:

$$I_{LR}(t) = 0 \tag{14}$$

$$V_{CR}(t) = \frac{I_{in}}{C_r} (t - t_2) + V_o \cdot \cos w_r(t_2 - t_1) \tag{15}$$

Mode 4 [freewheeling] ( $t_3 \leq t \leq T_s$ ): In this mode, the capacitor voltage is clamped to the output voltage, and the diode resumes conduction. This leads to the (16) and (17):

$$I_{LR}(t) = 0 \tag{16}$$

$$V_{CR}(t) = V_o \tag{17}$$

At the end of this mode, at time  $t = T_s$ , the cycle repeats. In Figure 8, the theoretical waveforms of the resonant tank are presented. Figure 8 shows the current and voltage for the ZCS approach for control voltage  $V_{gs}$  (Figure 8 (a)), capacitive voltage  $V_{cr}$  (Figure 8 (b)), and inductor current  $I_{LR}$  (Figure 8 (c)).

The voltage conversion ratio,  $M$ , of the quasi-resonant (ZCS) converter can be articulated through the application of the principle of energy conservation in the (18):

$$M = [1 - \frac{f_n}{2\pi} (\frac{M}{2Q} + 2\pi \sin^{-1}(\frac{M}{Q}) + \frac{Q}{M} (1 - \sqrt{1 - (\frac{M}{Q})^2}) )]^{-1} \tag{18}$$

Thus, the plotting of the conversion ratio  $M$  against normalized frequency is conducted in this study for different load values  $Q$ . The control characteristic is illustrated in Figure 9. The parameters for the ZCS-QRC discussed earlier are conveniently summarized in Table 3.

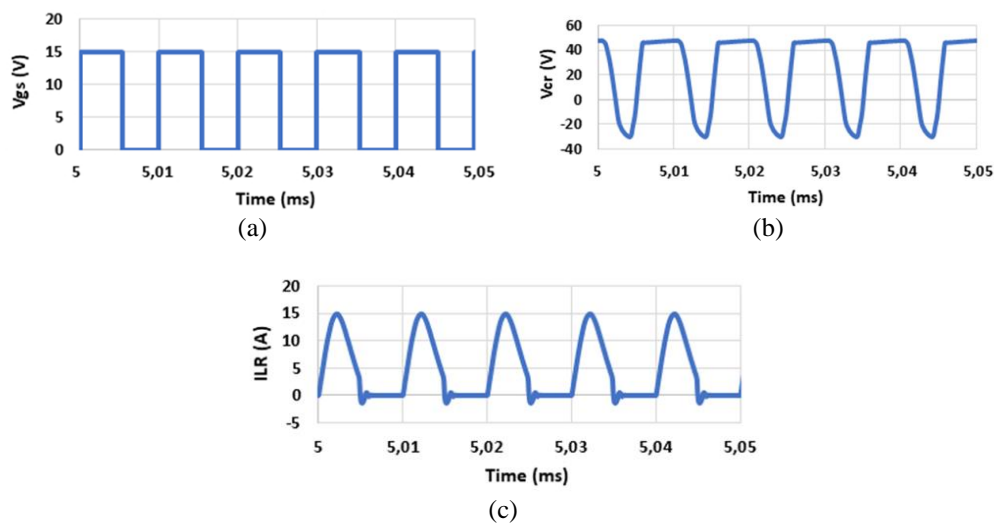


Figure 8. Current and voltage for the ZCS approach for (a) control voltage  $V_{gs}$ , (b) capacitive voltage  $V_{cr}$ , and (c) inductor current  $I_{LR}$

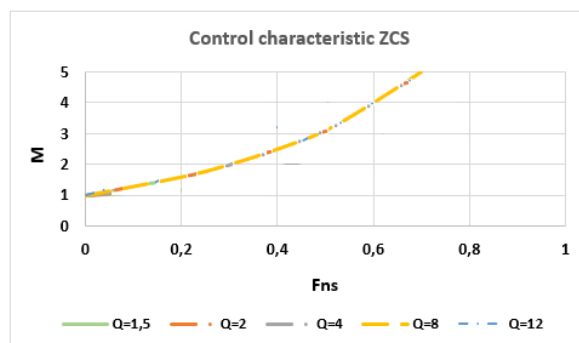


Figure 9. Conversion ratio characteristic as a function of normalized load



Table 3. Customizing the ZCS-QRC boost converter configuration

Parameter	Normalized value
Inductance $L_r$	4.7 uH
Capacitance $C_r$	150 nF
Resonant frequency $F_r$	198 KHz
Duty cycle D	~0.46

4. SIMULATION RESULTS AND DISCUSSION

4.1. Conducted electromagnetic interference assessment in boost converter systems: a quantitative analysis

The boost converter's impact on conducted-mode electromagnetic disturbances is significant. The switching cell represents the disruptive element that promotes current and voltage gradients, subsequently contributing to the generation of EMI that propagates through conduction within the frequency range [150 KHz, 30 MHz] (Figure 10). To assess these interferences, a line impedance stabilization network (LISN) is commonly used (Figure 10(a)). Serving as a filter between the tested boost converter and the power supply network, the LISN effectively isolates the power supply from the equipment under test, which can create disturbances in common mode and differential mode, as illustrated in Figure 10(b).

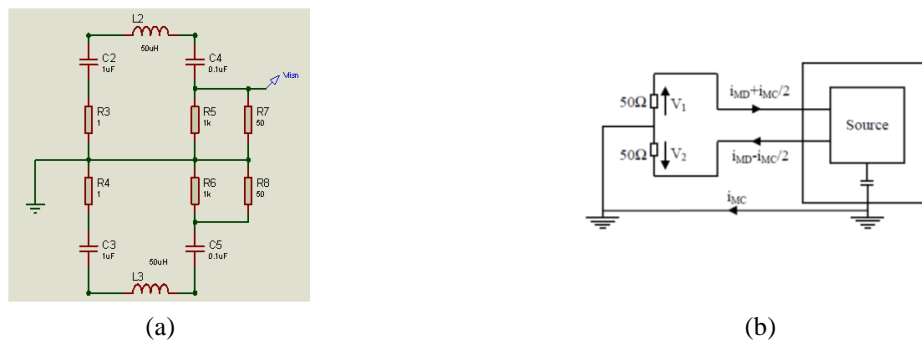


Figure 10. Conducted electromagnetic emission measurements by means of (a) a LISN device for both and (b) common and differential modes

This segment of the study conventionally involves the quantification of conducted-mode EMI [21], [22], specifically for the standard boost converter whose features have been detailed earlier. The configuration of the employed chopper encompasses a power source, a conducted emissions measurement device (LISN), a control architecture, and a switching cell integrated with a filter and a resistive output load (refer to Figure 11). It is noteworthy that the voltage  $V_{lisn}$  recorded across the LISN serves as a representation encapsulating both differential and common-mode disturbances [23].

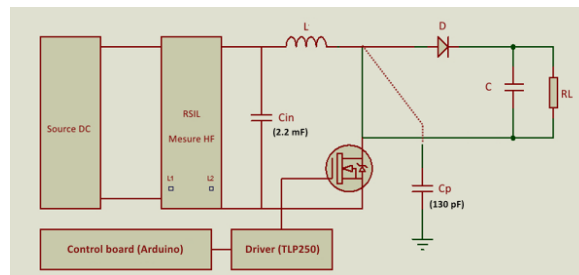


Figure 11. The testing framework for conducted emissions in a boost converter

In crafting the simulation framework for the model illustrated in Figure 11, we employed the Isis Proteus environment, incorporating the parameters detailed in Table 1. Our analysis was primarily centered on the spectral composition of voltage  $V_{lisn}$ , serving as an indicator of disturbances in both differential and



common modes. Our principal objective revolved around the mitigation of the frequency components within this voltage, with particular emphasis on reducing the power spectral density, specifically within the frequency range spanning from 10 kHz to 30 MHz [24]. The ensuing section delves into an in-depth investigation of the envisaged methodologies, namely ZVS and ZCS, and their respective efficiencies in curtailing the electromagnetic disturbances propagated by the typical boost converter operating under Hard switching conditions. The simulation results are presented in Figure 12, especially in Figure 12(a) the results of the ZVS approach, and Figure 12(b) the results of the ZCS approach.

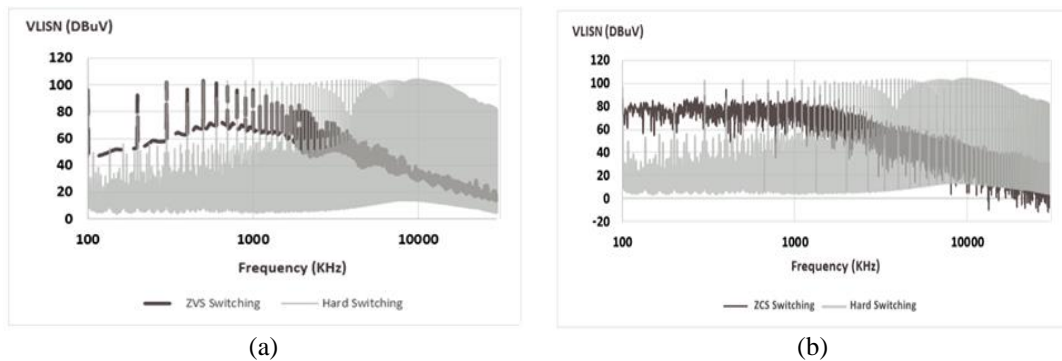


Figure 12. Frequency analysis of voltage ( $V_{lisn}$ ) for (a) ZVS and (b) ZCS approach

The simulation findings emphasize the discernible merits associated with soft switching methodologies, specifically both ZVS and ZCS, with respect to the amelioration of conducted electromagnetic disturbances. The ZVS switching technique, as delineated in Figure 12(a), excels in the considerable mitigation of the high-frequency spectrum attributable to its smooth transitions, thereby attenuating abrupt voltage fluctuations. Practically, this approach ensures that the voltage across the switches remains proximate to zero during the switching process, thereby mitigating swift voltage transitions and suppressing the generation of high-frequency harmonics.

In contradistinction to conventional hard switching techniques, the utilization of both ZVS and ZCS methodologies presents considerable advantages in terms of electromagnetic compatibility and interference reduction [25]. This distinction is particularly noteworthy in Figure 12(b), where the efficacy of ZCS switching becomes apparent at lower frequencies by minimizing current spikes during switching transitions. This deliberate strategic approach is directed towards mitigating disturbances stemming from abrupt alterations in current, a critical endeavor in managing emissions within lower frequency ranges. The inherent attributes of ZVS and ZCS position them as promising choices for the effective control of conducted electromagnetic disturbances. When implemented, these techniques not only enhance the quality and integrity of electrical signals but also prove instrumental in high-performance applications that demand strict adherence to electromagnetic performance standards.




## 5. CONCLUSION

In summary, this study demonstrates the efficacy of ZVS and ZCS techniques in mitigating EMI in EV boost converters. These methods significantly reduce power spectral density within the [10 kHz, 30 MHz] frequency range, enhancing electromagnetic compatibility. ZVS is engineered with a primary focus on attenuating high-frequency EMI through the facilitation of seamless transitions in voltage. In parallel, ZCS is meticulously crafted to diminish abrupt spikes in current at lower frequencies. The conspicuous superiority exhibited by both ZVS and ZCS in comparison to conventional hard-switching methodologies signifies a compelling prospect for heightened operational efficiency and broader integration within the specialized domain of power electronics for EVs. These findings establish a solid foundation for improving reliability and efficiency in EV power electronics. For future work, exploring machine learning algorithms for real-time adaptive control of ZVS and ZCS parameters is recommended. Investigating synergies between advanced control strategies and switching techniques can optimize EMI mitigation. Additionally, studying scalability for different power levels and EV architectures will offer insights for widespread implementation in the automotive industry, advancing this critical technology.




## REFERENCES

- [1] A. Rabie, A. Ghanem, S. S. Kaddah, and M. M. El-Saadawi, "Electric vehicles based electric power grid support: a review," *International Journal of Power Electronics and Drive Systems (IJPEDS)*, vol. 14, no. 1, pp. 589–605, Mar. 2023, doi: 10.11591/ijpeds.v14.i1.pp589-605.
- [2] S. Feng and C. L. Magee, "Technological development of key domains in electric vehicles: Improvement rates, technology trajectories and key assignees," *Applied Energy*, vol. 260, p. 114264, Feb. 2020, doi: 10.1016/j.apenergy.2019.114264.
- [3] L. Fakhfakh, A. Alahdal, and A. Ammous, "Fast modeling of conducted EMI phenomena using improved classical models," in *2016 Asia-Pacific International Symposium on Electromagnetic Compatibility (APEMC)*, IEEE, May 2016, pp. 549–552. doi: 10.1109/APEMC.2016.7522795.
- [4] A. A. E. B. A. El-Halim, E. H. E. Bayoumi, W. El-Khattam, and A. M. Ibrahim, "Electric vehicles: a review of their components and technologies," *International Journal of Power Electronics and Drive Systems (IJPEDS)*, vol. 13, no. 4, p. 2041, Dec. 2022, doi: 10.11591/ijpeds.v13.i4.pp2041-2061.
- [5] M. Al, J. Van, and H. Gualous, "DC/DC converters for electric vehicles," in *Electric Vehicles - Modelling and Simulations*, InTech, 2011. doi: 10.5772/17048.
- [6] R. Redl, "Power electronics and electromagnetic compatibility," in *PESC Record. 27th Annual IEEE Power Electronics Specialists Conference*, IEEE, pp. 15–21. doi: 10.1109/PESC.1996.548553.
- [7] K. M. Muttaqi and M. E. Haque, "Electromagnetic interference generated from fast switching power electronic devices," *International Journal of Innovations in Energy Systems and Power*, vol. 3, no. 1, pp. 19–26, 2008.
- [8] P.-C. Chen, W.-C. Lin, M.-C. Tsai, G.-C. Hsieh, and H.-I. Hsieh, "Analysis, simulation and design of soft-switching mechanisms in DC to DC step-down converter," in *2019 IEEE 4th International Future Energy Electronics Conference (IFEEEC)*, IEEE, Nov. 2019, pp. 1–5. doi: 10.1109/IFEEEC47410.2019.9015023.
- [9] Z. M'barki and K. Senhaji Rhazi, "Optimization of electromagnetic interference conducted in a devolver chopper," in *Proceedings of the 2nd International Conference on Electronic Engineering and Renewable Energy Systems. ICEERE 2020. Lecture Notes in Electrical Engineering*, Singapore: Springer, 2021, pp. 523–529. doi: 10.1007/978-981-15-6259-4\_55.
- [10] A. Ali, J. Chuanwen, M. M. Khan, S. Habib, and Y. Ali, "Performance evaluation of ZVS/ZCS high efficiency AC/DC converter for high power applications," *Bulletin of the Polish Academy of Sciences Technical Sciences*, pp. 793–807, Jul. 2020, doi: 10.24425/bpasts.2020.134185.
- [11] J. L. Kotny, T. Duquesne, and N. Idir, "Design of EMI filters for DC-DC converter," in *2010 IEEE Vehicle Power and Propulsion Conference*, IEEE, Sep. 2010, pp. 1–6. doi: 10.1109/VPPC.2010.5729047.
- [12] Z. M'barki, Y. Mejdoub, K. S. Rhazi, and K. Sabhi, "Implementing pseudo-random control in boost converter: an effective approach for mitigating conducted electromagnetic emissions," *Indonesian Journal of Electrical Engineering and Informatics (IJEI)*, vol. 11, no. 3, Sep. 2023, doi: 10.52549/ijeie.v11i3.4832.
- [13] Z. M'barki, K. S. Rhazi, and Y. Mejdoub, "A proposal of structure and control overcoming conducted electromagnetic interference in a buck converter," *International Journal of Power Electronics and Drive Systems (IJPEDS)*, vol. 13, no. 1, pp. 380–389, Mar. 2022, doi: 10.11591/ijpeds.v13.i1.pp380-389.
- [14] Z. M'barki, K. S. Rhazi, and Y. Mejdoub, "Practical implementation of pseudo-random control in step-down choppers and its efficiency in mitigating conducted electromagnetic emissions," in *Artificial Intelligence and Smart Environment. ICAISE 2022. Lecture Notes in Networks and Systems*, Cham: Springer, 2023, pp. 674–682. doi: 10.1007/978-3-031-26254-8\_98.
- [15] K. Shipra, S. N. Sharma, and R. Maurya, "Passivity-based controllers for ZVS quasi-resonant boost converter," *IET Control Theory & Applications*, vol. 14, no. 20, pp. 3461–3475, Dec. 2020, doi: 10.1049/iet-cta.2020.0129.
- [16] Z. M'barki, K. Senhaji Rhazi, and Y. Mejdoub, "A novel fuzzy logic control for a zero current switching-based buck converter to mitigate conducted electromagnetic interference," *International Journal of Electrical and Computer Engineering (IJECE)*, vol. 13, no. 2, pp. 1423–1436, Apr. 2023, doi: 10.11591/ijece.v13i2.pp1423-1436.
- [17] Fang Lin Luo and Hong Ye, "Investigation of EMI, EMS and EMC in power DC/DC converters," in *The Fifth International Conference on Power Electronics and Drive Systems, 2003. PEDS 2003.*, IEEE, pp. 572–577. doi: 10.1109/PEDS.2003.1282904.
- [18] M. Laour, R. Tahmi, and C. Vollaie, "Modeling and analysis of conducted and radiated emissions due to common mode current of a buck converter," *IEEE Transactions on Electromagnetic Compatibility*, vol. 59, no. 4, pp. 1260–1267, Aug. 2017, doi: 10.1109/TEMPC.2017.2651984.
- [19] Z. M'barki, A. A. Salih, Y. Mejdoub, and K. S. Rhazi, "Enhancing conducted EMI mitigation in boost converters: a comparative study of ZVS and ZCS techniques," in *Artificial Intelligence, Data Science and Applications. ICAISE 2023. Lecture Notes in Networks and Systems*, Cham: Springer, 2024, pp. 434–441. doi: 10.1007/978-3-031-48573-2\_62.
- [20] A. Farhadi and A. Jalilian, "Modeling and simulation of electromagnetic conducted emission due to power electronics converters," in *2006 International Conference on Power Electronic, Drives and Energy Systems*, IEEE, Dec. 2006, pp. 1–6. doi: 10.1109/PEDES.2006.344331.
- [21] K. Khotimah, Y. Yoppy, M. I. Sudrajat, V. Permatasari, E. Trivida, and T. A. W. Wijarnoko, "Conducted emission investigation of infant incubator heating control mode," *International Journal of Electrical and Computer Engineering (IJECE)*, vol. 12, no. 6, pp. 5900–5910, Dec. 2022, doi: 10.11591/ijece.v12i6.pp5900-5910.
- [22] L. Zhai, T. Zhang, Y. Cao, S. Yang, S. Kavuma, and H. Feng, "Conducted EMI prediction and mitigation strategy based on transfer function for a high-low voltage DC-DC converter in electric vehicle," *Energies*, vol. 11, no. 5, p. 1028, Apr. 2018, doi: 10.3390/en11051028.
- [23] B. Nassireddine, B. Abdelber, C. Nawel, D. Abdelkader, and B. Soufyane, "Conducted EMI prediction in DC/DC converter using frequency domain approach," in *2018 International Conference on Electrical Sciences and Technologies in Maghreb (CISTEM)*, IEEE, Oct. 2018, pp. 1–6. doi: 10.1109/CISTEM.2018.8613398.
- [24] G. Minardi, G. Greco, G. Vinci, S. A. Rizzo, N. Salerno, and G. Sorbello, "Electromagnetic simulation flow for integrated power electronics modules," *Electronics*, vol. 11, no. 16, p. 2498, Aug. 2022, doi: 10.3390/electronics11162498.
- [25] S. Deshmukh (Gore) et al., "Review on classification of resonant converters for electric vehicle application," *Energy Reports*, vol. 8, pp. 1091–1113, Nov. 2022, doi: 10.1016/j.egy.2021.12.013.




**BIOGRAPHIES OF AUTHORS**

**Zakaria M'barki**    was born in Morocco in 1990. He is a Ph.D. student at the Laboratory of Networks, Computing Science, Telecommunication, and Multimedia (RITM), ESTC Casablanca, Hassan 2 University in Morocco. In 2014, he graduated with honors from Morocco's National School of Electricity and Mechanics with a degree in electrical and telecommunication engineering. His current research interests are 'renewable energy sources', 'power systems, and 'electromagnetic compatibility'. He can be contacted at email: mbarki.ensem@gmail.com.






**Ali Ait Salih**    is a Ph.D. student at the Laboratory of Networks, Computing Science, Telecommunication, and Multimedia (RITM), ESTC Casablanca, Hassan 2 University in Morocco. Current research interests are: 'power electronics' and 'electromagnetic compatibility'. He can be contacted at email: aitsalihali@gmail.com.



**Youssef Mejdoub**    was born in Morocco, in 1980. He received his Ph.D. thesis on the modeling of multiconductor transmission Lines, in 2014 from Cadi Ayyad University, Marrakech Morocco. Since 2016, he has been a Professor at the Superior School of Technology (EST), University of Hassan II of Casablanca. His current research interests are 'antennas', 'electromagnetic compatibility', and 'MTL lines'. He can be contacted at email: ymejdoubec@yahoo.fr.



**Kaoutar Senhaji Rhazi**    qualified professor in electrical engineering; at the School of Technology in Casablanca. Morocco. A graduate engineer in electrical engineering from the Mohammadia School of Engineers (EMI) in Rabat. Morocco (in 1991). Passed academic qualification in the same field in 2014. Became a higher education teacher in 2020. Current research interests are: 'power electronics' and 'electromagnetic compatibility'. She can be contacted at email: senhaji.ksree@gmail.com.